Available online at www.sciencedirect.com
ScienceDirect
Journal of Power Sources 165 (2007) 660–665
JOURNAL OF POWER SOURCES
www.elsevier.com/locate/jpowsour

Short communication

Preparation and characterization of *o*-$LiMnO_2$ cathode materials

She-huang Wu *, Ming-tlau Yu

Department of Materials Engineering, Tatung University, 40 Chungshan N. Road, Sec. 3, Taipei 104, Taiwan

Available online 28 November 2006

Abstract

Small particle-sized orthorhombic $LiMnO_2$ powders were prepared via Pechini's route with Li/Mn molar ratio ranging between 1.00 and 1.20, followed by calcinations at 300 °C in air and heat-treatment at temperatures between 700 and 900 °C for various durations under flowing nitrogen. The effects of heat-treatment conditions and starting Li/Mn molar ratio on the crystalline structure and the electrochemical properties were investigated with XRD, SEM, and capacity retention study. Orthorhombic phase were found exclusively in the samples prepared with starting Li/Mn molar ratios between 1.00 and 1.05 followed by heat-treatment at 800 °C for 15 h, whereas monoclinic Li_2MnO_3 and tetragonal $Li_2Mn_2O_4$ were also observed in the samples prepared with Li/Mn ratios higher than 1.10. The charge/discharge curves of capacity retention studies and the cyclic voltammograms showed that the transformation of *o*-$LiMnO_2$ into cycle-induced spinel phase proceeds more progressively and the capacity loss upon cycling are more significant for the samples containing the impurity phases than the well-ordered *o*-$LiMnO_2$ sample. The sample synthesized with starting Li/Mn ratio of 1.05 followed by heat treatment at 800 °C for 15 h showed the most promising cycling performance among the prepared powders with the maximum discharge capacity of 158 mAh g^{-1} at 20th cycle and capacity loss of 3% between 20th and 80th cycles at 30 °C.
© 2006 Elsevier B.V. All rights reserved.

Keywords: Orthorhombic lithium manganese oxide; Pechini method; Lithium battery; Cathode material

1. Introduction

Lithium ion batteries have become important power sources for portable electronics, such as notebook computers, cellular phones, and digital cameras. Due to the high cost and safety issues of the currently used cathode material, $LiCoO_2$, many efforts have been done to look for the alternative cathode materials. Among the promising candidates of the cathode materials for secondary lithium batteries, such as $LiMn_2O_4$ [1–3], $LiNi_{0.8}Co_{0.2}O_2$ [4–6], $LiNi_{1/3}Co_{1/3}Mn_{1/3}O_2$ [7,8], $LiFePO_4$ [9], and $LiMnO_2$ [10–12], layer $LiMnO_2$ shows advantages in cost, safety, and high theoretical capacity of 285 mAh g^{-1} which is twice of spinel $LiMn_2O_4$ for the same Mn^{4+}/Mn^{3+} redox couple [13,14]. However, layer $LiMnO_2$ suffers from its capacity loss due to the phase transformation to spinel-like phase upon cycling [15,16]. Although, orthorhombic $LiMnO_2$ also exhibits phase transformation into spinel-like $Li_xMn_2O_4$ upon cycling, orthorhombic $LiMnO_2$ was proved to show good cycleability [10–12].

o-$LiMnO_2$ materials have generally been prepared by a solid state reaction methods by heating the mixtures of manganese oxides and lithium salts under inert atmosphere at high temperatures [17–21] or heating an equimolar mixture of γ-MnOOH and LiOH at temperatures between 300 and 450 °C under dry nitrogen or argon [21,22]. Wet chemical processes of ion exchange [23], hydrothermal [24,25], sol–gel [26], and reverse-microemulsion [27] methods were also applied to synthesize *o*-$LiMnO_2$. However, the electrochemical behavior of the *o*-$LiMnO_2$ is greatly dependent on the synthetic route. Although Croguence et al. showed that small crystallite size and stacking faults in the crystal structure are important for the electrochemical activity of *o*-$LiMnO_2$ [18,28]. Jang et al. reported *o*-$LiMnO_2$ materials with high capacities and good cycling stability were prepared by firing homogeneous precursor in a reduced oxygen partial pressure atmosphere to give samples with small crystallite size but a low content of stacking faults [16]. They suggested that Jahn Teller transformation is suppressed by cation disorder and the formation of nanodomains structure, which provides an elasticity to accommodate the orthorhombic-spinel transformation strains and anisotropic change in volume arising from cycling a highly ordered material prepared by high temperature synthesis route. Moreover, Lee et al. manifested that grinding

* Corresponding author. Tel.: +886 2 25922458; fax: +886 2 25936897.
E-mail address: shwu@ttu.edu.tw (S.-h. Wu).

0378-7753/$ – see front matter © 2006 Elsevier B.V. All rights reserved.
doi:10.1016/j.jpowsour.2006.10.044

treatment can promote the cycling capacity and activate the initial lithium insertion-extraction of high-temperature prepared well-defined *o*-$LiMnO_2$ powders at 3 V region [29]. Therefore, the electrochemical behaviors of *o*-$LiMnO_2$ cathode materials are significantly dependent on the crystalline size, particle size, and size distribution.

Though the high temperature prepared *o*-$LiMnO_2$ materials generally have better cycling stability over 3 and 4 V regions than those prepared at low temperatures, they often have large particle size and show rate capability limitations. Grinding can reduce the average particle size of the prepared powders, however, impurities and defects may also be introduced to degrade the electrochemical properties of the prepared *o*-$LiMnO_2$ powders. In the presentation, well-crystallized *o*-$LiMnO_2$ powders of small particle size were prepared via Pechini's route. The electrochemical properties of the as-prepared *o*-$LiMnO_2$ for lithium ion batteries are presented herein.

2. Experimental

o-$LiMnO_2$ powders were prepared via Pechini's route that was illustrated elsewhere [30,31], with Li/Mn molar ratio ranging between 1.00 and 1.20. Then the precursors were calcined at 300 °C in air for 6 h and heat-treated at temperatures between 700 and 900 °C under flowing nitrogen for 10–20 h followed by oven cooling to room temperature. The compositions of the resulting powders were analyzed by using an inductively coupled plasma spectrometer (ICP-OES, Optima 2100DV, Perkin-Elmer, USA). The powder X-ray diffraction (XRD 6000, Shimazu, Japan) using Cu Kα radiation was employed to identify the crystalline phase of the prepared powders. The particle morphologies of the resulting samples were observed with a scanning electron microscope (SEM, JSM 5600, Hitachi, Japan).

The sample electrodes for the electrochemical studies were made by blending the prepared powders with acetylene black and polyvinylidene fluoride (PVDF) with weight ratio of 83:10:7 in *N*-methyl pyrrolidone (NMP), then the resultant slurries were coated onto Al-foil substrate, followed by heating at 110 °C for 24 h, punching into disk electrodes (10.0 mm in diameter), pressing, and heating again at 110 °C for 8 h. Thus prepared electrodes with about 2 mg active material were used as the working and the cathode electrodes for assembling three-electrode and CR2032 coin-type cells with lithium as anode, counter, and reference electrodes, Celgard 2400 as separator, 1M $LiPF_6$ in EC-DEC (1:1 by volume) as electrolyte in an argon filled glove box. The three-electrode cells were used for cyclic voltammetry (CV) studies by connecting with a potentiostat/galvanostat (Voltalab PGZ-402, Radiometer Analytical, France) and scanned at 0.1 mV s^{-1} rate between voltage limits of 2.5 and 4.5 V. The capacity retention studies were performed by cycling the CR2032 coin-type cells at current rate of 0.1*C* (about 0.03 mA) with cutoff voltages of 2.5 and 4.3 V at 30 and 50 °C.

3. Results and discussion

The XRD patterns of the samples prepared by calcinations at 300 °C in air for 6 h followed by heat-treatment at various temperatures for 15 h with starting Li/Mn molar ratio of 1.05 are shown in Fig. 1. It is found that orthorhombic $LiMnO_2$ forms in the sample heat-treated at 700 °C in company with monoclinic Li_2MnO_3 and tetragonal $Li_2Mn_2O_4$. The diffraction peaks corresponding to the orthorhombic structure become prominent and the peak intensities increase with heat-treatment temperature as the samples were heat-treated at temperatures between 700 and 800 °C. Orthorhombic phase is observed exclusively without other second phase in the sample heat-treated at 800 °C. As can be seen in Fig. 1, the sharp (1 1 0) peak depicts that the 800 °C prepared *o*-$LiMnO_2$ via the Pechini's route is considered to have well-ordered orthorhombic structure. From further conformation with Rietveld refinement, the lattice parameters of $a = 4.573(7)$, $b = 5.750(5)$, and $c = 2.804(2)$ Å were obtained with $R_p = 7.36\%$, $\chi^2 = 2.54(3)$, $R_{wp} = 6.45\%$. These results agree well with those synthesized by other methods reported in the literatures and the structure of the prepared powder belong to the space group *Pmnm* [12,24,27,29]. In the 900 °C sample, spinel $LiMn_2O_4$ is observed in addition to the orthorhombic phase. It may be attributed to the Li loss in the sample that was proved by the Li/Mn molar ratio of 0.97 in the prepared powder analyzed with ICP. The SEM photographs of the powders prepared at various temperatures with Li/Mn molar ratio of 1.05 are shown in Fig. 2. It is found that the particle size increases slightly to 200 nm in diameter as the heat-treatment temperature increases from 700 to 800 °C, however, sintered particles with diameters of 2 ~ 3 μm are observed in the 900 °C sample. These values are larger than those of the powders prepared by other wet chemical methods [26,27].

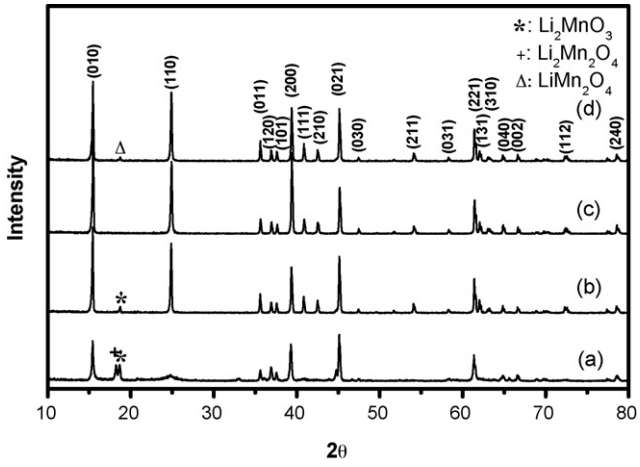

Fig. 1. The XRD patterns of the powders prepared with starting Li/Mn molar ratio of 1.05 by calcinations at 300 °C for 6 h in air and then heat-treatment at various temperatures for 15 h under flowing nitrogen: (a) 700 °C; (b) 750 °C; (c) 800 °C; (d) 900 °C.

Fig. 3 shows the XRD patterns of the powders prepared with various starting Li/Mn molar ratios and then calcined at 300 °C in air for 6 h followed by heat-treated at 800 °C for 15 h under flowing nitrogen. While only orthorhombic phase is observed in the samples prepared with starting Li/Mn molar ratios of 1.00.and 1.05, monoclinic Li_2MnO_3 and tetragonal $Li_2Mn_2O_4$ are also found in the samples prepared with starting Li/Mn molar ratios of 1.10.and 1.20 that may be owing to the excess of Li in the

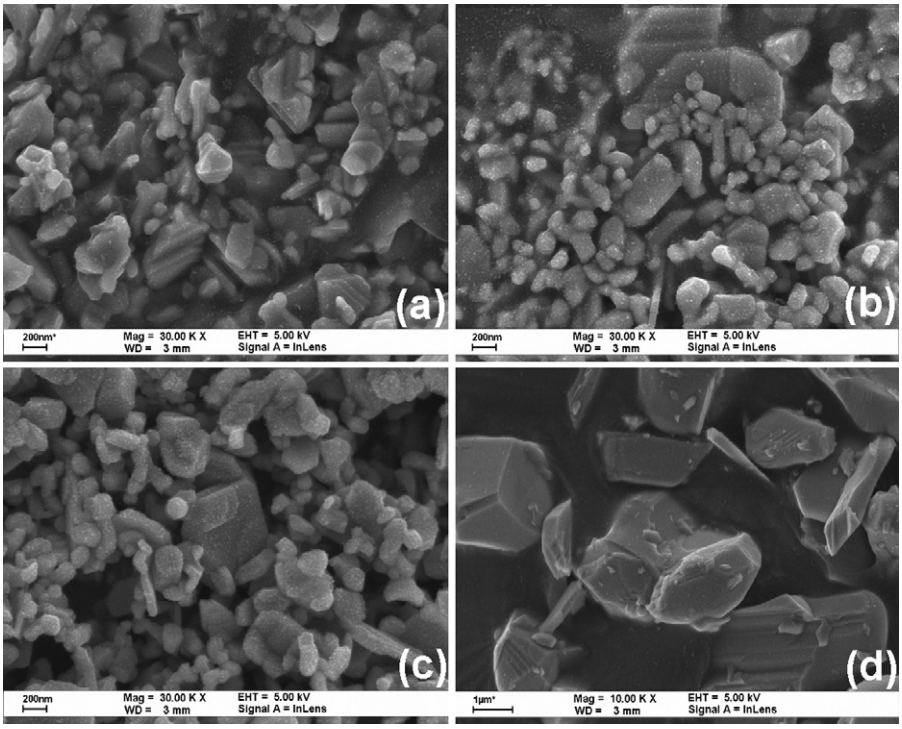

Fig. 2. The SEM photographs of the powders prepared with starting Li/Mn molar ratio of 1.05 by calcinations at 300 °C for 6 h in air and then heat-treatment at various temperatures for 15 h under flowing nitrogen: (a) 700 °C; (b) 750 °C; (c) 800 °C; (d) 900 °C.

powders. These high Li/Mn ratio samples exhibit high stacking faults in the structure that can be revealed from the broaden (1 1 0) peak in the XRD patterns shown as Fig. 3(c) and (d) [32]. The high stacking faults may be induced by the existence of Li_2MnO_3 and $Li_2Mn_2O_4$.

From the initial charge/discharge curves of the coin-type cells shown in Fig. 4, characteristic initial charge and discharge plateaus at 3.6 and 3.0 V of *o*-$LiMnO_2$ are found for the cells with cathodes prepared with Li/Mn = 1.00 and 1.05 as previously reported [18,22,24,25,29]. In Fig. 4(c) and (d), in addition to the charge and discharge plateaus of *o*-$LiMnO_2$, the charge plateau at 4.1 V and discharge plateau at 3.9 V are also observed for the samples prepared with Li/Mn = 1.10 and 1.20. That means the existence of tetragonal $Li_2Mn_2O_4$ in the samples and more spinel-like behavior is observed in the initial discharge process. The lowering of the characteristic initial charge plateau at 3.6 V to around 3.5 V may be caused by the existence of $Li_2Mn_2O_4$ [33]. As observed previously by Shu et al. [34], these materials also show large initial irreversible capacities due to the phase transformation from orthorhombic to spinel-like phase. It had been suggested by Thackeray that Li^+ ion de-lithiated from the octahedral sites on charging and the Mn^{3+} ions migrate from the octahedral sites to neighboring vacant octahedral sites at the same time, such that Li^+ ions cannot re-insert into the original octahedral sites and high irreversible capacity at initial cycle

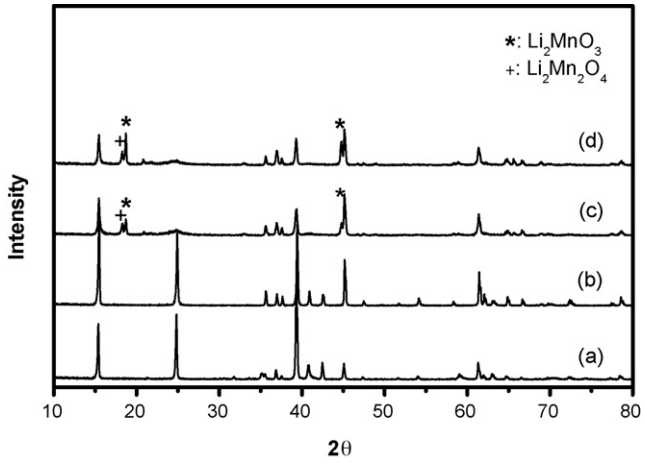

Fig. 3. The XRD patterns of the powders prepared by calcinations at 300 °C for 6 h in air and then heat-treatment at 800 °C for 15 h under flowing nitrogen with various Li/Mn molar ratios: (a) 1.00; (b) 1.05; (c) 1.10; (d) 1.20.

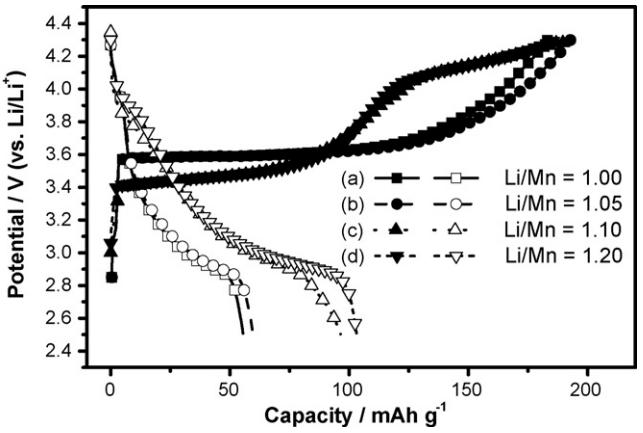

Fig. 4. Initial charge and discharge curves of the coin-type cells comprised with cathode prepared with various Li/Mn molar ratios. Cycling was carried out at 0.1*C* rate between 4.3 and 2.5 V at 30 °C.

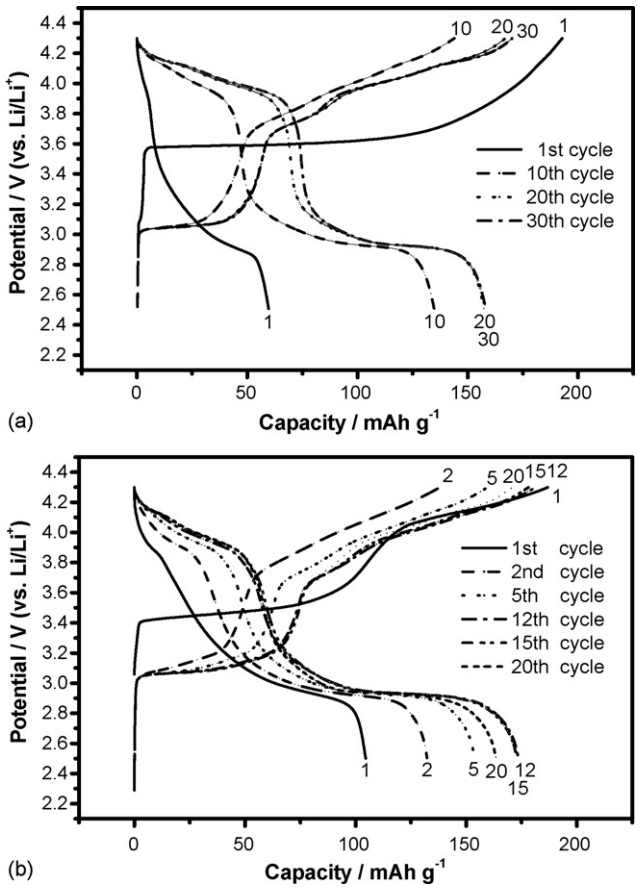

Fig. 5. The typical charge and discharge curves of the coin-type cells comprised with cathode prepared with various Li/Mn molar ratios: (a) 1.05; (b) 1.20. Cycling was carried out at 0.1*C* rate between 4.3 and 2.5 V at 30 °C.

was observed [14]. The existence of Li_2MnO_3 and $Li_2Mn_2O_4$ or stacking faults may accelerate the transformation that can be manifested by the charge/discharge curves shown in Fig. 5 and thus reduce the irreversible capacity of the initial cycle.

From the typical charge and discharge profiles, shown in Fig. 5(a), of the well-ordered sample prepared with starting Li/Mn molar ratio of 1.05, the length of the 4 and 3 V plateaus getting longer simultaneously for the initial cycles. The discharge capacities in the 4 and 3 V regions increase from 10 and 50 mAh g^{-1} for the first cycle to 70 and 88 mAh g^{-1} for the 20th cycle, respectively. With further cycling, the discharge capacity of the 4 V plateau increases further and becomes 75 mAh g^{-1}, while the capacity of the 3 V plateau decrease to 83 mAh g^{-1} after 30 cycles. Though no capacity loss was found during 20th and 30th cycles, reordering of Li^+ toward the cycle-induced spinel-like structure is in progress. For the sample prepared with Li/Mn molar ratio of 1.20, which exhibits high stacking faults, the phase transformation of the orthorhombic phase into spinel one is more progressive than the well-ordered *o*-$LiMnO_2$ sample. As shown in Fig. 5(b), the discharge capacities in 4 V and 3 V regions increase from 25 and 80 mAh g^{-1} for the first cycle to 60 and 115 mAh g^{-1} for the 12th cycle, respectively. The discharge capacities maintain at the same values till 15th cycle and then the capacity at 3 V region decreases to the value of 105 mAh g^{-1} after 20 cycles while the capacity at 4 V remains

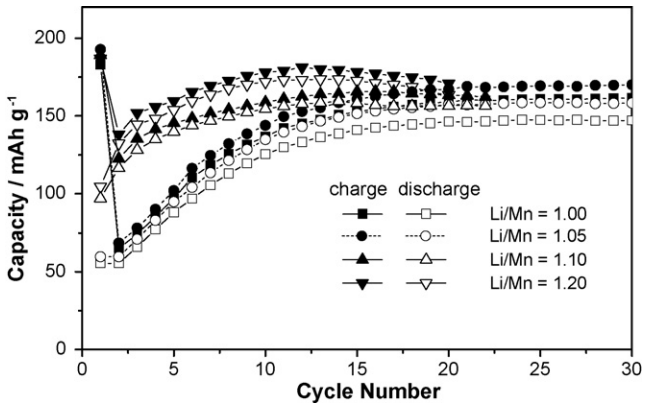

Fig. 6. The plot of charge and discharge capacities vs. number of cycles for the coin-type cells comprised with cathode prepared with various Li/Mn molar ratios. Cycling was carried out at 0.1*C* rate between 4.3 and 2.5 V at 30 °C.

unchanged. As reported previously [16,22,25], the capacity fading of the *o*-$LiMnO_2$ materials is mainly due to the loss in 3 V region, which may by caused by the collective Jahn-Teller distortion of cycle-induced spinel phase. The cycling performance of the samples prepared with various starting Li/Mn molar ratios are shown in Fig. 6. It is found that the samples with Li_2MnO_3 and $Li_2Mn_2O_4$ phases have lower initial irreversible capacities than the well-ordered *o*-$LiMnO_2$ samples, however, the second phases containing samples manifest higher capacity fade than the later. The capacity of the well-ordered *o*-$LiMnO_2$ samples increases upon cycling and becomes saturated after 20 cycles while the profiles of the samples prepared with starting Li/Mn ratios of 1.10 and 1.20 reach the maximum capacity at 12th cycle and the capacities decrease thereafter. The capacity loss is contributed predominantly by the fade around 3 V plateau as shown above.

The transformation of *o*-$LiMnO_2$ samples from orthorhombic into spinel-like phase upon cycling had been studied with ex situ and in situ XRD studies [16,25,27,35], and differential capacity plot [16,18,25]. The cyclic voltammetry can also be used to reveal the reactions occur during the transformation. Fig. 7 shows the cyclic voltammograms performed at a scan rate of 0.1 mV s^{-1} over the potential range between 2.5 and

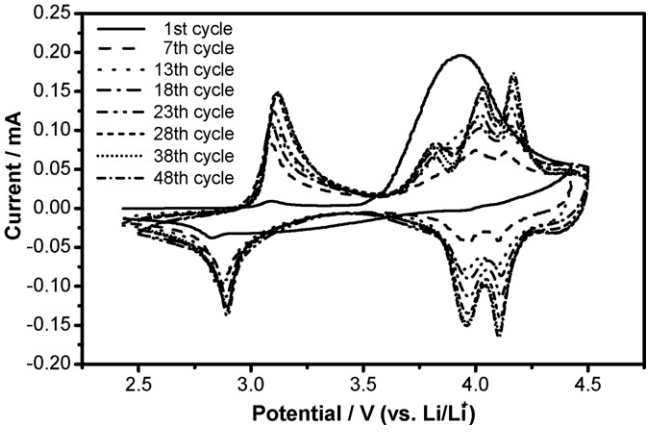

Fig. 7. Cyclic voltammograms of the *o*-$LiMnO_2$ prepared with Li/Mn molar ratio of 1.05 at 0.1 mV s^{-1} scanning rate between 2.5 and 4.5 V.

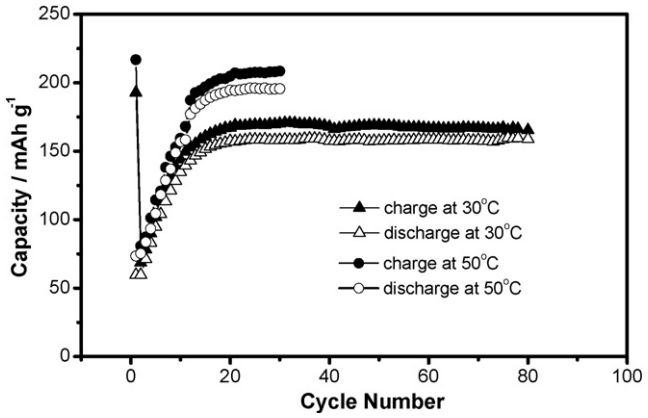

Fig. 8. Cycling performance of well-ordered *o*-$LiMnO_2$ prepared with starting Li/Mn molar ratio of 1.05 at 30 and 50 °C.

4.5 V for the well-ordered sample prepared with starting Li/Mn molar ratio of 1.05. As the charge/discharge curves illustrated above, there are one distinct oxidation peak at 3.7 V, one indistinct oxidation peak at 3.1 V, and two vague reduction peaks at 2.6 and 3.9 V in the plot of first cycle. While the distinct peak at 3.7 V disappear, the redox peaks at 3 V become clear, and the redox peaks at 4 V appear in the second cycle. The characteristic redox peaks of spinel $LiMn_2O_4$ at around 3.95 and 4.10 V are observed in the plot of 7th cycle. The height of redox peaks around 3 and 4 V increase with cycling, indicating a progressive formation of cycle-induced spinel phase, and become saturated after 38 cycles. These results are in consistent with those shown in Fig. 5(a), though capacity saturation is found at higher cycle number than that obtained from capacity retention study. In addition to the characteristic redox peaks, the continuous appearance of an additional oxidation peak at 3.8 V on the cyclic voltammograms after 18 cycles but not in the reduction stage is observed. The appearance of the additional peak has been observed previously from the differential capacity plots [16,36]. Although its origin is unknown, it is probably due to the complicated electrochemically active reactions of cycle-induced spinel upon charging. It is also worthy to note that the 3 V redox reaction exhibits larger apparent polarization than the 4 V reactions that can be seen from the potential difference of the redox peaks.

Fig. 8 shows the cycling performance of the well-ordered *o*-$LiMnO_2$ powder prepared with starting Li/Mn molar ratio of 1.05 and heat-treated at 800 °C for 15 h. Maximum discharge capacity of 158 mAh g^{-1} after cycling 20 cycles and very low capacity loss of 3% between 20th and 80th cycles is obtained at 30 °C. It indicates that even though the well-ordered *o*-$LiMnO_2$ powder prepared by the Pechini's method transforms into spinel-like phase upon cycling and the discharge capacity increases during the initial cycles as those of the powders prepared with solid-state reaction and wet chemical methods [18,20,25,27], however, the cycle-induced spinel derived from the powder demonstrates less significant deterioration on the electrochemical properties after further cycling than those derived from powders prepared by wet chemical processes [22,25,26,27]. Like the results reported by Lee et al. [29], the sample exhibits even better cycling performance at 50 than at 30 °C with maximum discharge capacity of 190 mAh g^{-1}. That may be attributed to the enhancement of Li^+ ion diffusivity in the host by increasing operation temperature.

4. Conclusion

Well-ordered *o*-$LiMnO_2$ powders with small particle size can be prepared successfully by a Pechini's method with starting Li/Mn molar ratios of 1.00 and 1.05 followed by calcinations at 300 °C for 6 h and heat-treatment at 800 °C for 15 h under flowing nitrogen, while Li_2MnO_3 and $Li_2Mn_2O_4$ were also found in the samples prepared with Li/Mn higher than 1.10. The phase transformation of the orthorhombic phase into spinel one in the Li_2MnO_3 and $Li_2Mn_2O_4$ containing powders is more progressive and the capacity fading is also more significant than the well-ordered *o*-$LiMnO_2$ sample. The sample prepared with starting Li/Mn molar ratio of 1.05 shows maximum capacity of 158 mAh g^{-1} at 30 °C and 190 mAh g^{-1} at 50 °C after 20 cycles with very low capacity fading.

Acknowledgements

This work was financially supported by Tatung University and Tatung Company, Taipei, Taiwan.

References

[1] M.M. Thackeray, P.J. Johnson, L.A. De Picciotto, P.G. Bruce, J.B. Goodenough, Mater. Res. Bull. 19 (1984) 179.
[2] T. Ohzuku, M. Kitagawa, T. Hirai, J. Electrochem. Soc. 137 (1990) 769.
[3] J.M. Tarascon, D. Guyomard, Electrochim. Acta 38 (1993) 1121.
[4] F. Nobili, F. Croce, B. Scrosati, R. Marassi, Chem. Mater. 13 (2001) 1642.
[5] J. Ying, C. Wan, C. Jiang, Y. Li, J. Power Sources 99 (2001) 78.
[6] P. Periasamy, H.S. Kim, S.H. Na, S.I. Moon, J.C. Lee, J. Power Sources 132 (2004) 213.
[7] N. Yabuuchi, T. Ohzuku, J. Power Sources 119–121 (2003) 171.
[8] I. Belharouak, Y.K. Sun, J. Liu, K. Amine, J. Power Source 123 (2003) 247.
[9] K. Padhi, K.S. Nanjundaswamy, J.B. Goodenough, J. Electrochem. Soc. 144 (1997) 1188.
[10] I.J. Davidson, R.S. McMillan, J.J. Murray, J.E. Greedan, J. Power Sources 54 (1995) 232.
[11] A.J. Paterson, A.D. Robertson, P.G. Bruce, Electrochem. Solid-State Lett. 7 (2004) A331.
[12] M. Wu, Q. Zhang, H. Lu, A. Chen, Solid State Ionics 169 (2004) 47.
[13] P.G. Bruce, Chem. Commun. (1997) 1817.
[14] M.M. Thackeray, Prog. Solid State Chem. 25 (1997) 1.
[15] A.R. Armstrong, N. Dupre, A.J. Paterson, C.P. Grey, P.G. Bruce, Chem. Mater. 16 (2004) 3106.
[16] Y.I. Jang, B. Huang, H. Wang, D.R. Sadoway, Y.M. Chiang, J. Electrochem. Soc. 146 (1999) 3217.
[17] Y.I. Jang, Y.M. Chiang, Solid State Ionics 130 (2000) 53.
[18] L. Croguennec, P. Deniard, R. Brec, P. Biensan, M. Broussely, Solid State Ionics 89 (1996) 127.
[19] R.J. Gummow, D.C. Liles, M.M. Thackeray, Mater. Res. Bull. 28 (1993) 1249.
[20] I.J. Davidson, R.S. McMillan, I.J. Murray, J.E. Greedan, J. Power Sources 54 (1995) 232.
[21] T. Ohzuku, A. Ueda, T. Hirai, Chem. Express 7 (1992) 193.
[22] G. Pistoia, A. Antonini, D. Zane, Solid State Ionics 78 (1995) 115.
[23] I.N. Reimers, E.W. Fuller, E. Rossen, J.R. Dahn, J. Electrochem. Soc. 140 (1993) 3396.

[24] M. Tabuchi, K. Ado, C. Masquelier, I. Matsubara, H. Sakaebe, H. Kageyama, H. Kobayashi, R. Kanno, O. Nakamura, Solid State ionics 89 (1996) 53.
[25] S.T. Myung, S. Komaba, N. Kumagai, Electrochim. Acta 47 (2002) 3287.
[26] Z.P. Guo, K. Konstantinov, G.X. Wang, H.K. Liu, S.X. Dou, J. Power Sources 119–121 (2003) 221.
[27] C.H. Lu, H.C. Wang, J. Eur. Ceram. Soc. 24 (5) (2004) 717.
[28] L. Croguennec, P. Deniard, R. Brec, A. Lecerf, J. Mater. Chem. 5 (1995) 1919.
[29] Y.S. Lee, Y.K. Sun, K. Adachi, M. Yoshio, Electrochim. Acta 48 (2003) 1031.
[30] W. Lin, G.C. Farrington, F. Chaput, B. Dunn, J. Electrochem. Soc. 143 (1996) 879.
[31] S.H. Wu, H.J. Su, Mater. Chem. Phys. 78 (2002) 189.
[32] L. Croguennec, P. Deniard, R. Brec, A. Lecerf, J. Mater. Chem. 7 (1997) 511.
[33] C.S. Johnson, M.M. Thackeray, Electrochem. Soc. Proc. 2000-36 (2001) 47.
[34] Z.X. Shu, I.J. Davidson, R.S. McMillan, J.J. Murray, J. Power Sources 68 (1997) 618.
[35] I.M. Kötschau, J.R. Dahn, J. Electrochem. Soc. 145 (1998) 2672.
[36] S.T. Myung, S. Komaba, N. Kumagai, J. Electrochem. Soc. 149 (2002) A1349.